

# Mechanical setup for optical aperture synthesis for wide field imaging

Peter Giesen<sup>\*a</sup>, Bas Ouwerkerk<sup>a</sup>, Hedser van Brug<sup>a</sup>, Teun van den Dool<sup>a</sup>,  
Casper van der Avoort<sup>b</sup>

<sup>a</sup>TNO TPD, Stieltjesweg 1, 2628 CK Delft, The Netherlands

<sup>b</sup>Delft University of Technology, Delft, The Netherlands

## ABSTRACT

Homothetic mapping is a technique that combines the images from several telescopes so that it looks like as though they came from a single large telescope. This technique enables a much wider interferometric field of view than current techniques can provide. To investigate the feasibility, a research testbed is built known as Delft Testbed Interferometer (DTI). DTI simulates a configuration of three telescopes collecting light from a set of 3 stars. The stars are simulated by coupling light from a Xenon light source into three fibres, which illuminate a parabolic mirror. The light that is used has wavelengths of 500 nm - 800 nm. The light from the three telescopes will be combined in such a way that the beam arrangement in the pupil plane corresponds with the telescope arrangement and the Optical Path Difference (OPD) is minimized for the three beams.

To achieve white light fringes with high visibility, the mechanical testbed that is 2 m x 1 m x 0.5 m in size, requires stable mounting of components. This paper describes the mounting of the diamond turned off-axis parabolic mirrors of 200 mm in diameter and 240 mm flat mirrors; furthermore, it describes components like the telescopes and the active controllable components for repositioning of the beam arrangement.

Mechanisms were developed for alignment of piezo actuators and for delay lines. The delay lines can also be used to compensate pupil rotation.

Test results demonstrate that the test setup is highly stable for temperature as well as for airflow, although the system is placed in a non-thermally controlled lab. This allows measurements of nm, in presence of  $\mu\text{m}$  disturbances.

**Keywords:** Homothetic mapping, aperture synthesis, thermal stability, adjustable stable mounts, telescope, pupil reimaging.

## 1. INTRODUCTION

The resolution of a telescope is primarily determined by the diameter of its first mirror. Although telescope systems using an 8 m diameter primary mirror are operative, the desire to increase the resolution is high. Smaller details can be detected with a telescope with bigger diameter. Increasing the mirrors can be rather expensive, since the production of extremely large telescopes is rather complex. The effect of a large telescope can be generated by combining multiple telescopes to an interferometric array.

Combining multiple telescopes has been done for years using radio telescopes, and since a decade it is also possible to combine optical telescopes. Optical astronomical telescopes have the advantage over radio telescopes in that they can use a detector with many pixels, thus enabling the use of an extended field of view. This field of view can be used to observe multiple objects or be used to observe faint objects while tracking strong objects.

To combine two or more telescopes, the optical path difference of the signal must be controlled at nanometer scale. But controlling the on-axis ray, the optical path difference of the off-axis rays is not automatically correct. In 1990, Beckers [ref.2] already showed that it is essential to maintain the pupil configuration of the telescopes to be able to get a wide field of view. Only when preserving the pupil configuration like diameter and orientation at the telescopes and at the imaging part, the on-axis rays and the off-axis rays will have 'zero' OPD for all beams. This technique is called homothetic mapping.

Because of the importance of homothetic mapping, various concepts have been investigated by ESO in the period of 1990 to 1996, but were not viable and other imaging concepts have been chosen. The need for homothetic mapping

---

\* giesen@tpd.tno.nl; phone ++31 15 26 92033; fax ++31 15 26 92111; www.tpd.tno.nl

remains, to increase the resolution and field of view of the telescopes. Not only telescopes on earth like VLT-I require wide field imaging but also future space telescopes like the ESA's Darwin mission require homothetic mapping. TNO TPD developed a prototype of a homothetic system known as Delft Testbed Interferometer (DTI), which simulates the fusing of three different telescopes. The system is to prove the feasibility of homothetic mapping and is intended to be a test-bed system for scientific experiments in the field of multi aperture interferometry.

## 2. OPTICAL APERTURE SYNTHESIS

Optical aperture synthesis is to combine the light of multiple telescopes as if it comes from one telescope. Given the situation that the light of two telescopes must be combined like given in Figure 1, then the wave front of the light source reaches telescope T1 first. To reach interference between telescope T1 and T2, the path difference of the beams must be within the coherence length. For visible light, the optical path difference (OPD) must be within 1000 nm to obtain fringes, and to perform fringe contrast and fringe phase experiments, the OPD must be within 20 nm. Since the information of the light cannot be temporarily stored, the physical length of the light path of T1 must be lengthened by a delay line. This delay changes since the projected baseline ( $b \cdot \cos(\alpha)$ ) of the telescopes changes in time because of the rotation of the earth.

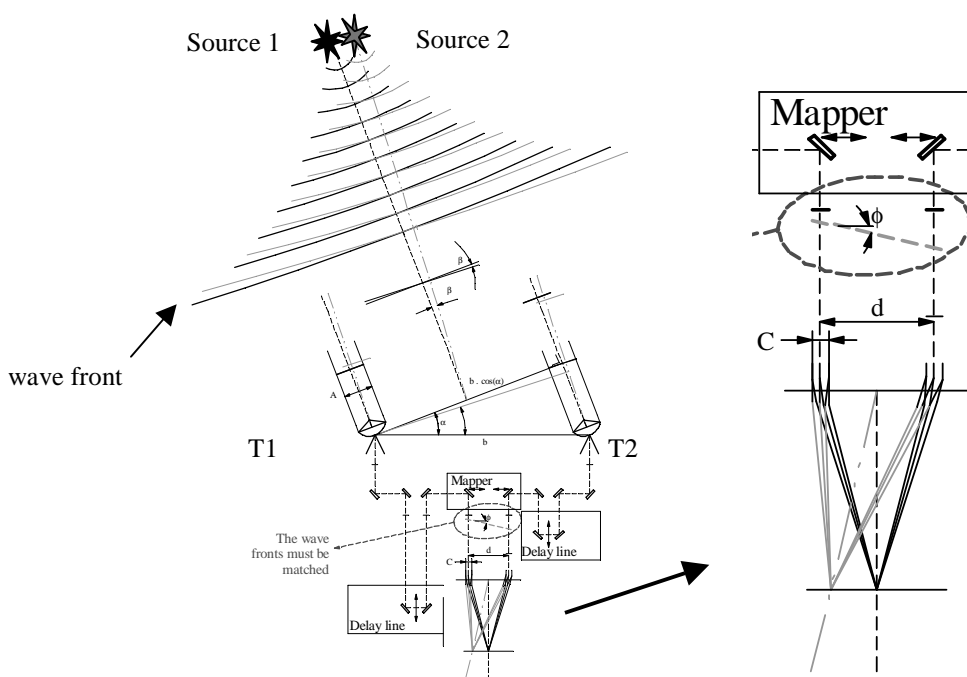


**Figure 1 Schematic setup of a telescope array with the wavefronts of two stars traced and imaged on the detector. To the right a detail the imaging of an off-axis source.**

Wide field imaging enables the measuring multiple objects at the sky. This is required to measure more accurately the distances between objects or measuring faint objects (science star) while controlling OPD of the telescope system using a much brighter source (reference star). Unfortunately, since the wave front of an off-axis source is tilted with respect to an on axis star, the OPD of the sources at the telescope is different as can be seen in Figure 1. This OPD difference cannot be corrected by the delay line at the same time. The OPD of the off axis star can be corrected by using a pupil mapper. A delay line positions the wave front in axial direction, the pupil mapper moves the wave front of the off-axis star in lateral direction, as is shown in Figure 1. To gain constructive interference in the whole field of view, the pupils must be corrected for OPD, position, rotation, and scaling. In this way, it is like the starlight travels through a masked-aperture imaging system.

### 3. SPECIFICATIONS

The prototype must represent a realistic setup for evaluating the requirements of homothetic mapping. Therefore the layout of the VLT-I telescope array is scaled by a factor 800 in DTI. This means that the beam diameter is smaller but the field of view is bigger. The accuracy and mapping principles are a good representation for the real VLT-I. This scaling will not imply the scaling of the prototype 800 times to be used in VLT-I since the beams of the telescopes can also be scaled. The specifications are given in Table 1.

At least three stars are required to assure a 2D field of view, and three telescopes are chosen for experiments to have 2 independent base lines.

Number of simulated stars	3 stars
Number of simulated telescopes	3 telescopes
Field of view	800 arcsec (scaled to ESO VLT-I: 1 arcsec)
Baseline	120 mm (scaled to ESO VLT-I: 100 m)
Beam diameter	10 mm (scaled to ESO VLT-I: 8 m)
Wavelength range	500 - 800 nm
Fringe phase measuring accuracy	Central $\lambda/25$

**Table 1 specifications of the DTI.**

To reach homothetic mapping at the given wavelength range and specifications given in Table 1, first, the differences between optical path lengths must be stable within 20 nm; second, the position of the beams at the mapping mirrors must be better than 10  $\mu\text{m}$ , and third, the angle between the beams looking to the same star, which is called pointing, must be smaller than 3  $\mu\text{rad}$  ( $=0.6$  arcsec) to ensure overlay of 90% of the Airy diameter of the three images.

Mapping accuracy, lateral	10 $\mu\text{m}$
Pointing accuracy	3 $\mu\text{rad}$
OPD accuracy	20 nm

**Table 2 specifications for homothetic mapping.**

### 4. OVERVIEW TEST SET UP

The DTI setup will be explained by the components in Figure 2. The setup covers a star simulator or sky simulator, a multiple telescope array, delay lines and pupil mapping, and an imaging part. DTI will simulate the configuration of three telescopes, each looking at the same three stars. The separated stars are simulated by coupling light of a xenon source, which is a white light source, into three single-mode fibers. The fibers illuminate a parabolic mirror (in Figure 2 represented as a lens), which reflect the light to an aperture plate representing the three telescopes. The delay lines and the pupil mappers guide the beams to the imager, which again is a parabolic mirror, but here in combination with a hyperbolic mirror, that images the stars onto a CCD camera. If the mapping is good, the Airy disks of the stars produced by the telescopes show fringes caused by interference of the beams.

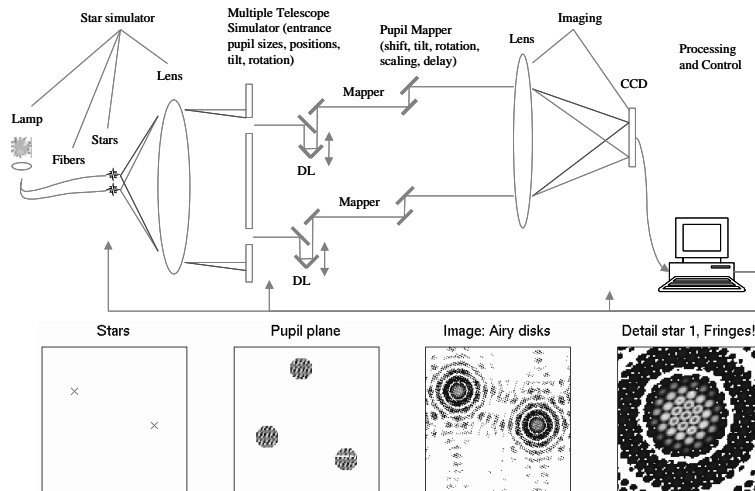


**Figure 2 layout of the setup, with simulated results.**

The results that will be obtained are shown in the simulation of the bottom section of Figure 2. Using a telescope with a pupil of limited size will result in an airy disk that is much bigger than the small dots of the image of the stars. Because of the fringe phase and the contrast in the airy disk that occurred due to the interference between the beams of the telescopes, e.g. the size of the stars can be determined. The research goal and the specifications to the optical design are given in reference's [4, 5, 6].

## 5. SUBSYSTEMS

In this section the subsystems of the setup are discussed. To achieve the nanometer accuracy and the flexibility to move elements across a vibration isolated optical table, the elements that have the same function e.g. delay lines are placed on a mounting block. After the beam splitting at the apertures, the three beams follow the separated paths through the setup, with separate mirrors and adjustment mechanisms. But, the global routing across the table is the same. Therefore, the effects of the global drift and expansion of the setup will be minimized. The OPD depends on the difference between the elements in the paths. The stability is achieved, by keeping the critical elements stable with respect to each other.

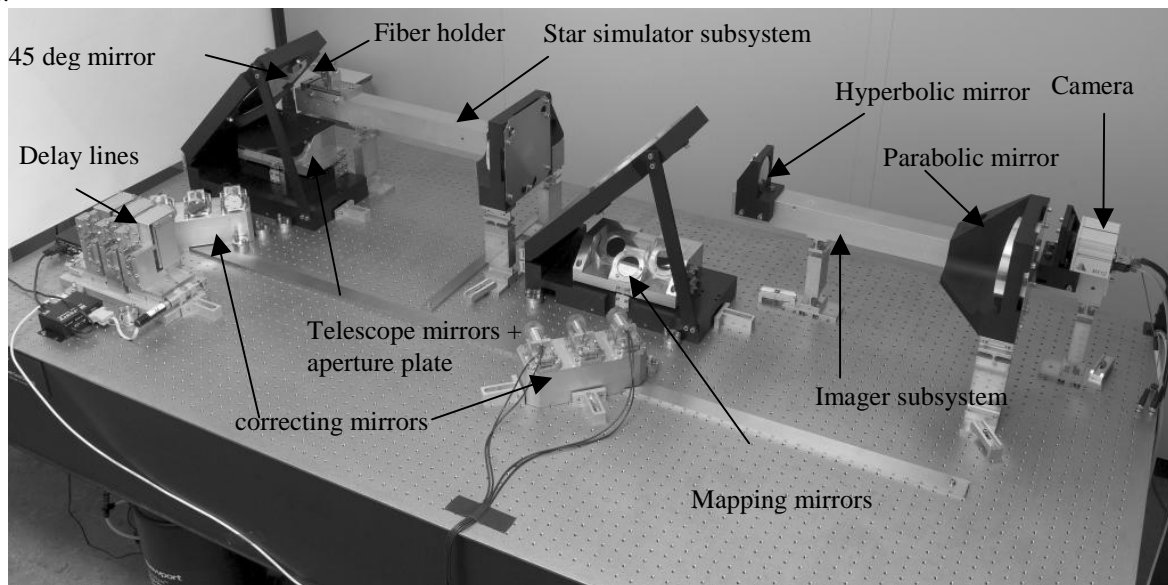


**Figure 3 Photograph of the DTI**

In the next paragraphs the mechanical highlights of the system are explained.

### 1. Star simulator

The star simulator consist of a fiber holder with 3 fibers. Two fibers are fixed to the mount, and the third fiber can move in vertical position using a micrometer screw or a linear motor. The light exits the fibers with an NA of 0.13 which illuminates the diamond turned parabolic mirror at a distance of 0.6 m. The fiber alignment holder can be moved in 6 degrees of freedom to be able to place the fiber into the focus of the parabolic mirror, and to aim the light at the mirror. In Figure 4 the alignment mechanism is shown. The 6 degrees of freedom can be adjusted using 6 adjustment screws.

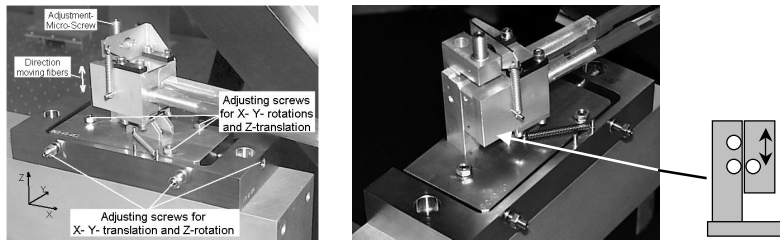


**Figure 4 Fiber alignment.**

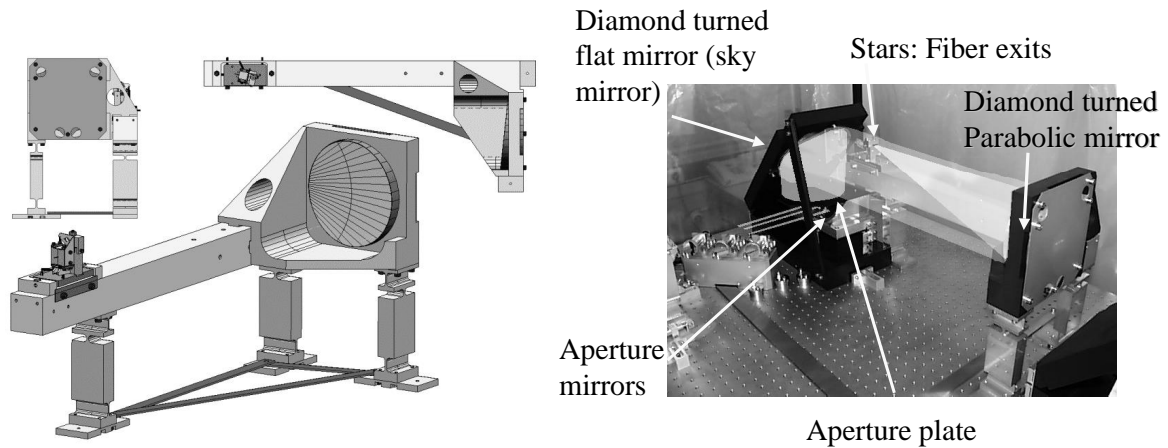


**Figure 5 Star simulator assembly. Left the CAD model, to the right a photograph including the light beam drawn from the stars through the aperture plate.**

The mounting of the off-axis aluminium diamond-turned mirror is placed in a holder that is also made of aluminium. Also the bar on where the fiber holder is placed, is made of aluminium. If the temperature changes, the distance of the fiber holder scales with respect to the mirror, but the curvature of the mirror scales also with the same amount, in such a way that the fiber exits stay in focus of the mirror. The aluminium setup can be placed on a stainless steel optics table because of the flexures that can take care of the difference in thermal expansion of the table and the setup. The flexures that are placed in this configuration that it provides a statically determined suspension of bar. Therefore, the bar is mounted stress free on the table and it provides an uniform thermal expansion if the temperature of the laboratory changes. The advantage is that the light coming form the parabolic mirror is always a parallel beam with the same pointing, independent on temperature. [ref 1, 3]

### 2. Telescopes

A diamond turned flat mirror (S1) is placed with an angle of 45 degree, to reflect the light coming from the parabolic mirror to the telescopes. Below the mirror the light will be blocked by an aperture plate with 3 holes of the three

telescopes. The mounting of the S1 mirror is placed on a intermediate body to cope with the difference in thermal expansion coefficient of the table and the S1 support, as is shown in Figure 6.

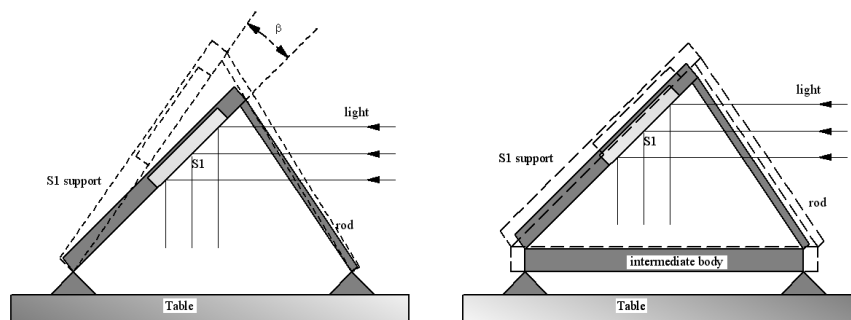


**Figure 6** The use of a intermediate body prevent tilting due to thermal expansion /drift of the 45 degree mirror.

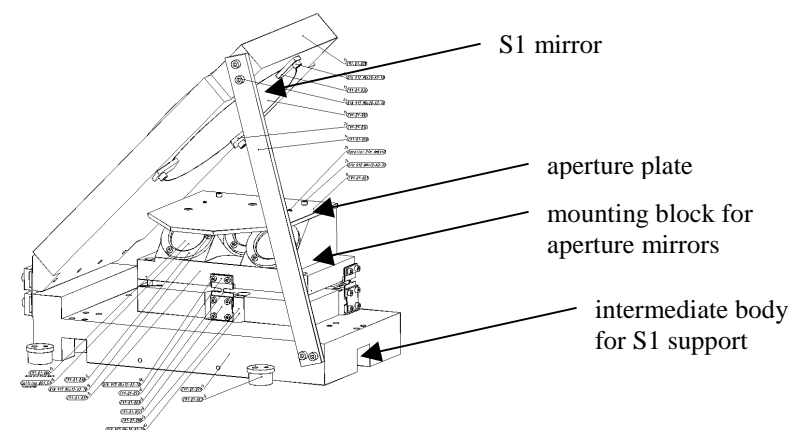


**Figure 7** The aperture plate and aperture mirrors are placed under the S1 mirror

The parallelism of the surfaces of the three aperture mirrors must be  $< 100 \mu\text{rad}$ . This could be met by manufacturing tolerances. A similar block is made for the mapping mirrors, see Figure 13.

### 3. Delay line

The function of the delay lines is to take care of the pathlength alignment errors of the components in the three paths. The required resolution is  $\mu\text{m}$  scale, since the OPD can be controlled at nanometer scale by actuation the correcting mirrors with a piezo actuator. The delay lines are adjustable in two axes of rotation. One axis is used for alignment; the second is to eliminate beam rotation. Two of the delay lines are placed on a motorized translation slide for OPD adjustment of  $1 \mu\text{m} - 12 \text{mm}$ . The third delay line is stationary.

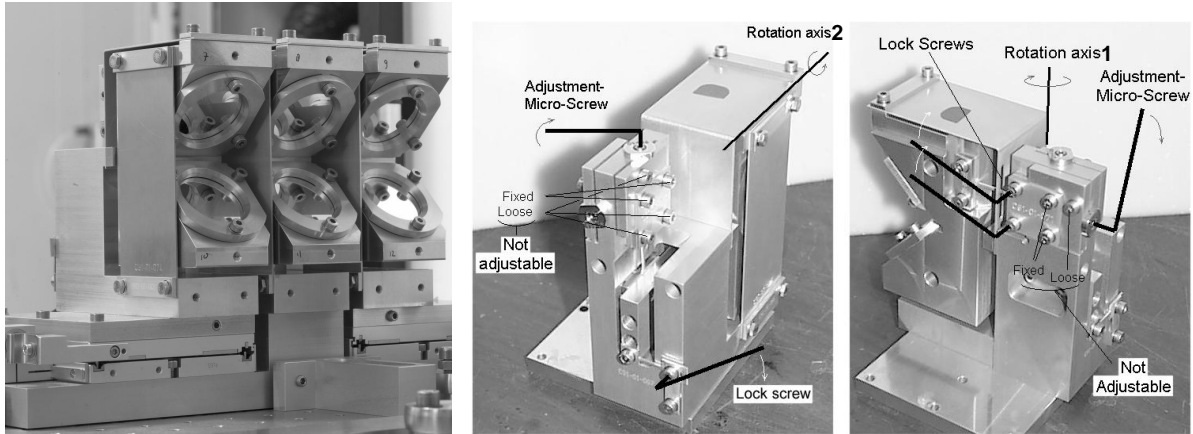


**Figure 8 Photograph of the delay lines. Right the to axis of rotation are shown and the adjustments. Rotation axis 2 is to adjust beam rotation, rotation axis 1 is to adjust beam alignment.**

#### 4. Mapping concept

To map the three individual beams to the right position, the beams can be translated according to the principle given in Figure 9. The correcting mirrors are placed on a tip/tilt/piston piezo actuator that can adjust the beam pointing in 2 directions. It can shift the beam in 2 directions, and even the OPD can be controlled at nanometer range.

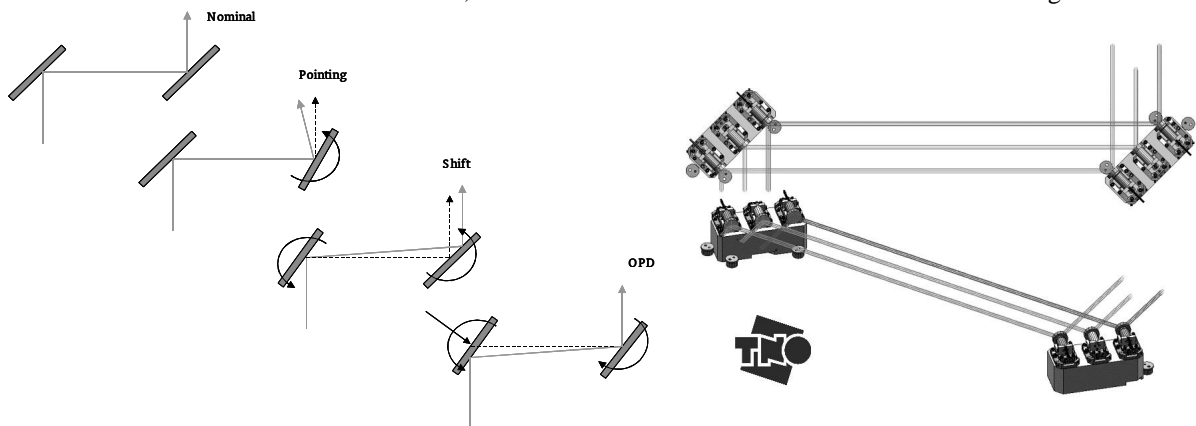


**Figure 9 The left picture shows the mapping principles, to the right the paths of the 3 beams are shown.**

The mapping mirrors are sensitive for OPD with respect to each other. Therefore mirrors are placed on a mount block and the front surfaces of the mirrors are placed in the same plane as is illustrated in Figure 10.

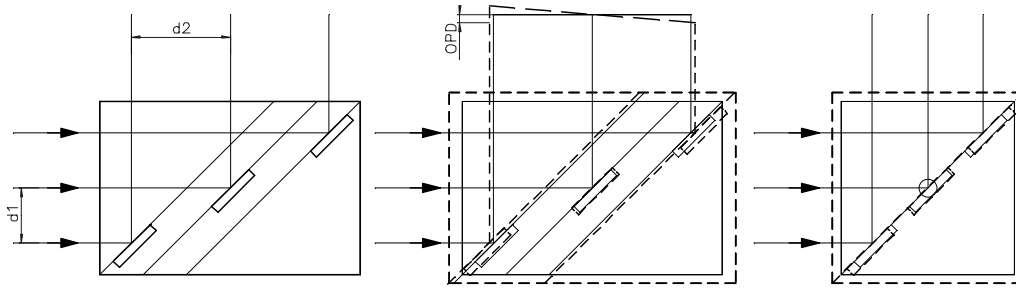


**Figure 10** If the mirrors are not mounted in the same plane, the OPD and the Mapping changes if the temperature changes. But if the mirrors are placed in the same plane, the thermal expansion has no effect.

To prevent uncontrolled sliding of the aluminium mount block across the optical table made of steel, the block is positioned on 3 contacts, and is pushed with springs to 3 alignment disks. The mounting block is statically determined [ref 1, 3], because all the contacts support one degree of freedom, and thus all the 6 degrees of freedom are constraint. The geometry of the alignment disks result in a centre of thermal expansion TC at the indicated spot (see Figure 12), of the aluminium mounting block with respect to the steel table top.

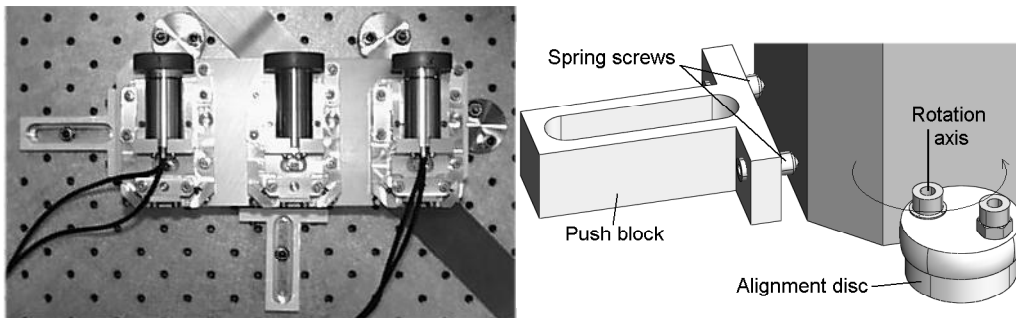


**Figure 11** Mapping mirrors are mounted together to a mounting block.

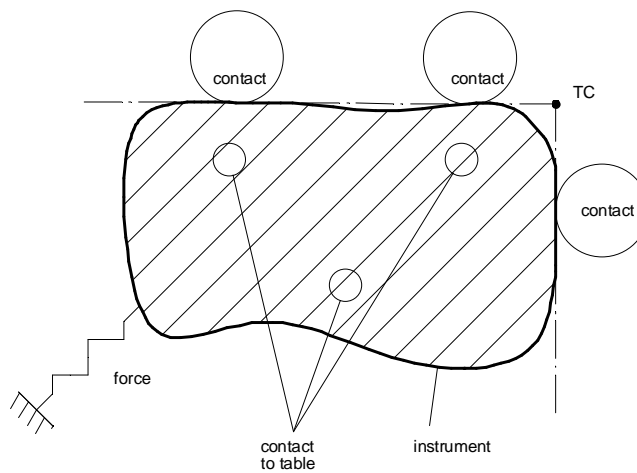


**Figure 12** Alignment of mounting block.



After the beams have been corrected for position, pointing and OPD, they are directed to the mapping mirrors shown in Figure 13. After the mapping mirrors, the 3 beams follow the same path to the imager.

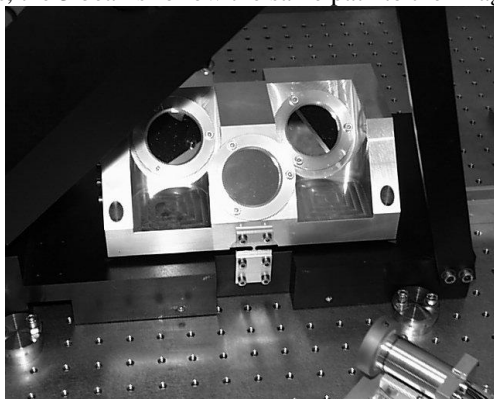


**Figure 13 Mapping mirrors. The pupil positions are formed on these mirrors.**

### **5. Imager subsystem.**

The imager is designed according to the same concept of the star simulator assembly. The subsystem consists of an aluminum off-axis parabola, an aluminum hyperbolic mirror and a CCD camera. The components are placed on an aluminum bar. The camera stays in focus of the imager subsystem even if the temperature changes.

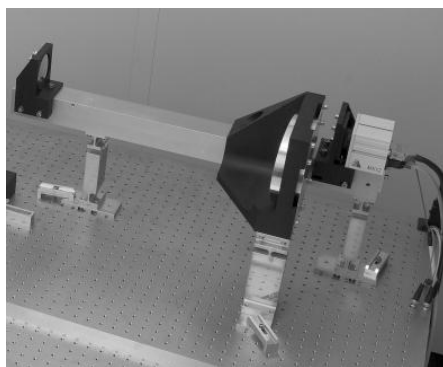


**Figure 14 Imager subsystem**

## **6. MEASUREMENTS**

The delay lines and the piezo actuators for the mapping can be controlled via a computer user interface in MATLAB<sup>®</sup>. The camera image can be used to perform measurements for mapping algorithms, which will not be discussed. In Figure 15 the camera image of the three stars is given. To the right, the fringes within a single star are shown. The amount of fringes is related to the wavelength range of the light source, and the angles of the fringe patterns represent the baseline configuration of the three telescopes.

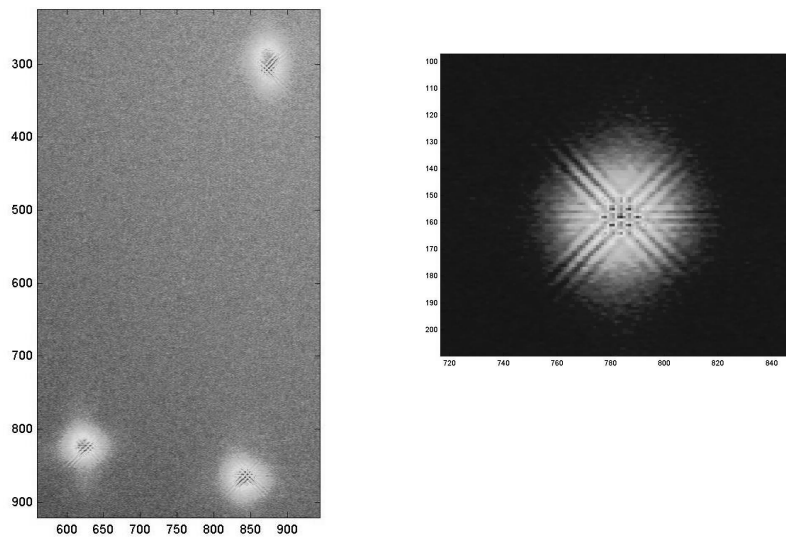


**Figure 15 Camera view of the 3 stars and a close-up of one star.**

### 7. STABILITY MEASUREMENTS

The test setup performs very well, although the setup is placed in a not-temperature controlled lab. The stability is tested over a night in open loop. In Figure 16 the drift of the beam pointing directions on the CCD is given. It shows the x and y position of the three beams which do not overlap to be able to measure at the same time. It shows a major change at nine pm, which could be related to the climate control of the building and automatically closing of the doors at nine o'clock. Although this seems dramatic, the drift 40 micrometer corresponds to a pointing drift of  $8 \mu\text{rad}$  in the system, since the imager that has a focal length of 5 meter. The drifts of the individual beams are much less, so that the image overlap is ensured. Improvements like a box around the setup, and minimizing the draught via the laboratory doors is going to be implemented.

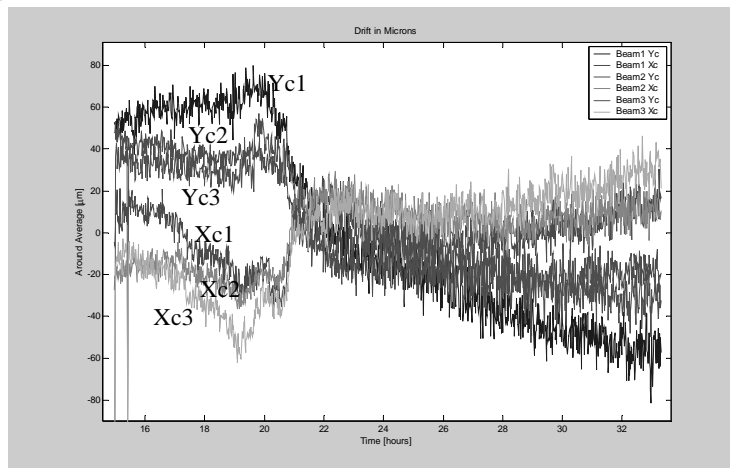


**Figure 16 Drift of the beam positions in time at the CCD, with sub-pixel resolution. 24 Hours means the start of a next day**

The OPD stability in open loop is tested by measuring the fringe movement of the three stars with two telescope beams (see Figure 17). The fringe movement is about half a fringe, which is 2 pixels on the camera. As can be seen, the fringes

of the tree stars all move by the same amount. The OPD drift of the setup is without any active OPD control not exceeding 200 nm over a time span of 40 minutes. The largest drift is at the start of the measurement, which can be related to the movement of personnel near the setup. Ten minutes after leaving the room, the setup is does not exceed 100 nm over 30 minutes.

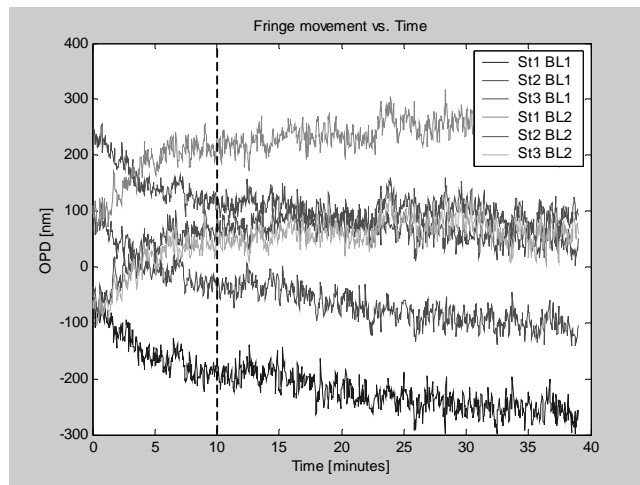


**Figure 17 Fringe movement in time with respect to a fixed camera pixel. The fringe drift is typically half a fringe, which is 2 pixels on the camera.**

To perform homothetic mapping, an OPD of 20 nm and a pointing accuracy of 3  $\mu$ rad is required as stated in Table 2. But the stability tests were performed open loop, and the measurements will be done in closed loop, so the stability is well met over the time span of a single measurement, which takes a few seconds. Also the mechanical and optical stability is passively that good, that the fringes remain until the next day, so with only minor corrections, the homothetic situation can be reached again. The correction will be done by the active controlled correction mirrors.

The passive stability of the setup is that good , that the overlap of the beams and the fringe visibility are well preserved.

## 8. ACKNOWLEDGEMENTS

The research for optical aperture synthesis is in cooperation with universities of Delft and Leiden, National Institute for Space Research (SRON), European Space Agency (ESA), and the European Southern Observatory (ESO). Apart from the work on DTI, other technologies for optical aperture synthesis include nulling interferometry and delay lines.

## 9. REFERENCES

1. M.P. Koster, *Constructieprincipes*, Twente University Press, Enschede, 2000.
2. J.M. Beckers, *The VLT Interferometer, III. Factors affecting wide field-of-view operation*, ESO Technical preprint no.16, March 1990.
3. Peter Giesen, Erik Folgering, *Design guidelines for thermal stability in opto-mechanical instruments*, Proc. SPIE **Vol. 5176** Optomechanics 2003
4. Hedser van Brug, et al, *Delft Testbed Interferometer- Layout design and reseach goals-*, Proc. SPIE **Vol. 4838** Interferometry for Optical Astronomy II, 2002
5. Hedser van Brug, et al, *Delft Testbed Interferometer: a homothetic mapping test setup*, Proc. SPIE **Vol. 5166** UV/Optical/IR space telescopes: Innovative Technologies and Concepts 2003
6. Bastiaan Oostdijck, et al, *Delft Testbed Interferometer: a homothetic mapping test setup*, European Optical Society, EOS Topical Meeting on Advanced Imaging Techniques, ISBN 3-00-012842-5, 2003